

Supplementary Material 2: Impacts of dehydration/hydration of algal cellulose fibrils on the IR spectra

Spatiotemporal dynamics of cellulose during enzymatic hydrolysis studied by infrared spectromicroscopy

Tina Jeoh^{1,*}, Jennifer Danger Nill^{1,2,§}, Wujun Zhao^{3,4,§}, Sankar Raju Narayanasamy^{3,5,§}, Liang Chen^{3,6}, and Hoi-Ying N. Holman^{3,*}

[§] These authors contributed equally to this manuscript

¹Biological and Agricultural Engineering, University of California Davis, Davis, CA

²Current: Amyris, Emeryville, CA

³Berkeley Synchrotron Infrared Structure Biology (BSISB), Lawrence Berkeley National Lab (LBNL), Berkeley, CA

⁴Current: Genus IntelliGen Technologies, Windsor, Wisconsin

⁵Current: Biosciences and Biotechnology Division, Physical and Life Science, Lawrence Livermore National Laboratory, Livermore, CA

⁶Current: TikTok, Mountain View, California

*Corresponding Authors

Initially hydrated cellulose was dried over the course of ~ 37 minutes in the microfluidics. Free/bulk water was evident as a broad peak at ~ 2150 cm^{-1} in the first 6 minutes, followed by fluctuations between 6 – 14 min, and complete absence after 14 min (Figure S2. 1A). Correspondingly, strong IR absorbance of the cellulose-associated water was evident at ~1650 cm^{-1} within the first 6 min, followed by drops in intensity between 6 – 14 min, and absence after 14 min (Figure S2. 1B). Accordingly, the impact of dehydration/hydration on the IR absorbance of the functional groups in cellulose was assessed by averaging the peak intensities and peak centers over the first 5 minutes as the fully hydrated state and between 25 – 35 min as the fully dry state of cellulose. Comparing the averages between hydrated and dried cellulose revealed some structural differences in cellulose influenced by the presence of absence of moisture.

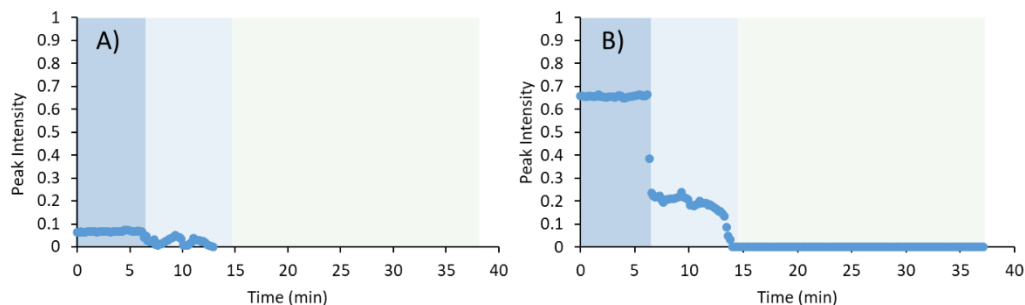


Figure S2. 1: Peak intensities of the free/bulk water peak centered at ~ 2150 cm^{-1} (A) and cellulose-associated water peak centered at ~ 1650 cm^{-1} (B).

Upon drying, the peak intensities of the C2-O2 vibration bands of cellulose decreased by ~ 16 – 19% upon drying (Figure S2. 1A and B), and the peak centers red-shifted from about 1113 to 1111 cm^{-1} ($\Delta = 2.2 \text{ cm}^{-1}$) and 1124 to 1123 cm^{-1} ($\Delta = 0.4 \text{ cm}^{-1}$) (Figure S2. 1C and D). In the hydrated state, the C2-O2 bonds resonate at higher frequency, indicating that interactions with water increases the prevalence and stiffen the C2-O2 bond. The dominant C2-O2 peak (1111 cm^{-1}), hypothesized to not participate in intra-fibril hydrogen bonding (Lee et al., 2015; Marechal & Chanzy, 2000), sees a larger frequency shift than the minor C2-O2 peak (1123 cm^{-1}) suggesting the influence of hydrogen bonding with water on the stiffness of this bond.

The C3-O3 vibration peak intensity decreased by ~ 22% upon drying, and the peak center shifted to lower frequency, from an average of 1059 to 1057 cm^{-1} (Figure S2. 3). These trends are similar to the influence of water on the C2-O2 vibration peak. Thus, similar to the C2-O2 bond, the C3-O3 bond increase in prevalence and stiffens in the presence of water. The C3-O3H participates as a donor in the hydrogen bonding interactions with the ring oxygen (O5) of the neighboring glucose residue. Exposure to water likely increases the frequency of these hydrogen bonds at the cellulose/water interface.

The C6-O6 bond in cellulose can take on one of three minimum energy rotameric conformations (Jarvis, 2023) that can be seen as three absorption bands at ~ 997, 1013, and 1033 cm^{-1} (Figure S2. 4). Based on the peak intensities, the 1033 cm^{-1} peak is the most dominant form, followed by the 1013 cm^{-1} , and the 997 cm^{-1} peaks. The intensities of the peaks at 997 and 1013 cm^{-1} peaks increase when dried, while the 1033 cm^{-1} peak intensity is not impacted by the hydration state (Figure S2. 4A, B, and C). All three C6-O6 vibration peaks red-shift to lower frequencies when dried (Figure S2. 4D, E, and F). These trends indicate that any of the C6-O6 rotamers are stiffer when hydrated, but the rotamers that resonate at 997 and 1013 cm^{-1} are less prevalent in the wet state. The ratio of average peak intensities of the 1033/1013/997 cm^{-1} peaks were approximately 6:2:1 in the wet state and 2:1.5:1 in the dry state, indicating that there is a strong preference for the rotamer that absorbs at 1033 cm^{-1} in the wet state. In cellulose I, C6-O6 predominantly occupies the *tg* rotameric form, where it can readily participate as an acceptor in the intramolecular hydrogen bond with C2-O2H of the neighboring glucose residue. The *gg* rotamer favors hydrogen bonding with water, while the *gt* rotamer is favored in vacuum (Newman & Davidson, 2004; Viëtor et al., 2002). The dominance of the 1033 cm^{-1} peak, and the non-influence of water on its stiffness suggests that this peak corresponds to the *tg* rotamer. The 1013 cm^{-1} and 997 cm^{-1} are presumed to correspond to the *gg* and *gt* rotamers, respectively, based on their expected abundance in hydrated cellulose.

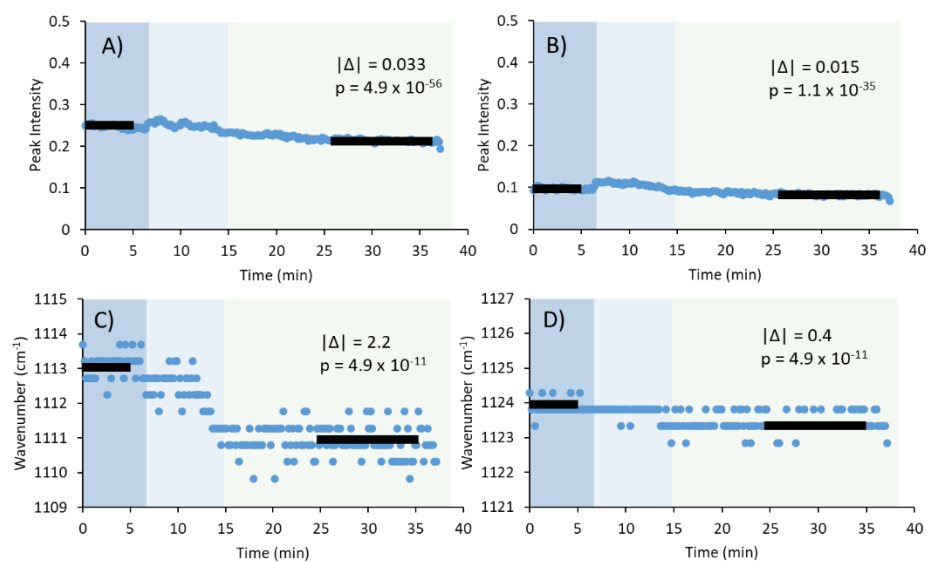


Figure S2. 2: C2-O2 in cellulose absorbs maximally near $\sim 1112 \text{ cm}^{-1}$ (A and C) and $\sim 1124 \text{ cm}^{-1}$ (B and D). The peak intensities (A and B) and wavenumber at peak center (C and D) are plotted over the observation time. Dark bars indicate averaged regions. Absolute differences between the averaged regions ($|\Delta|$) and the p -value indicating the t -statistic of the difference are shown ($p < 0.01$ are considered significant). Colored regions corresponding to Figure S2.1 indicate fully hydrated (dark blue), drying (light blue) and fully dried (green) periods in the experiment.

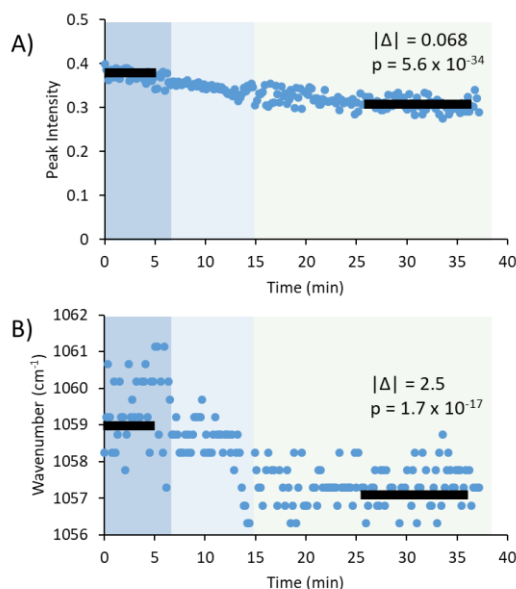


Figure S2. 3: C3-O3 of cellulose absorbs maximally $\sim 1059 \text{ cm}^{-1}$. The peak intensities (A) and wavenumber at peak center (B) are plotted over the observation time. Dark bars indicate averaged regions. Absolute differences between the averaged regions ($|\Delta|$) and the p-value indicating the t-statistic of the difference are shown ($p < 0.01$ are considered significant). Colored regions corresponding to Figure S2.1 indicate fully hydrated (dark blue), drying (light blue) and fully dried (green) periods in the experiment.

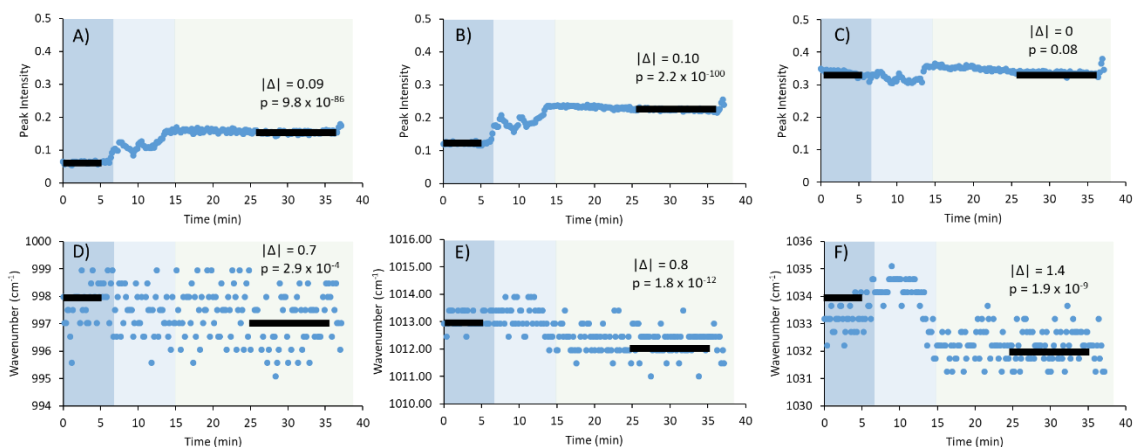


Figure S2. 4: C6-O6 of dry cellulose absorbs maximally ~ 998 , 1013 , and 1033 cm^{-1} . The peak intensities (A, B, and C) and wavenumber at peak center (D, E, and F) are plotted over the observation time. Dark bars indicate averaged regions. Absolute differences between the averaged regions ($|\Delta|$) and the p-value indicating the t-statistic of the difference are shown ($p < 0.01$ are considered significant). Colored regions corresponding to Figure S2.1 indicate fully hydrated (dark blue), drying (light blue) and fully dried (green) periods in the experiment.

The glycosidic bond peaks at around 1161 and 1205 cm^{-1} , and the anomeric C1-O1 vibration peaks were minimally impacted by changes in the hydration state of cellulose (Figure S2. 5). The only detectable change due to hydration was a $\sim 17\%$ increase in average intensity of the 1161 cm^{-1} absorption peak.

Notably, in the dry state, the peak center of the 1153 cm⁻¹ band exhibited significantly greater variability around the averaged position (Figure S2. 5F).

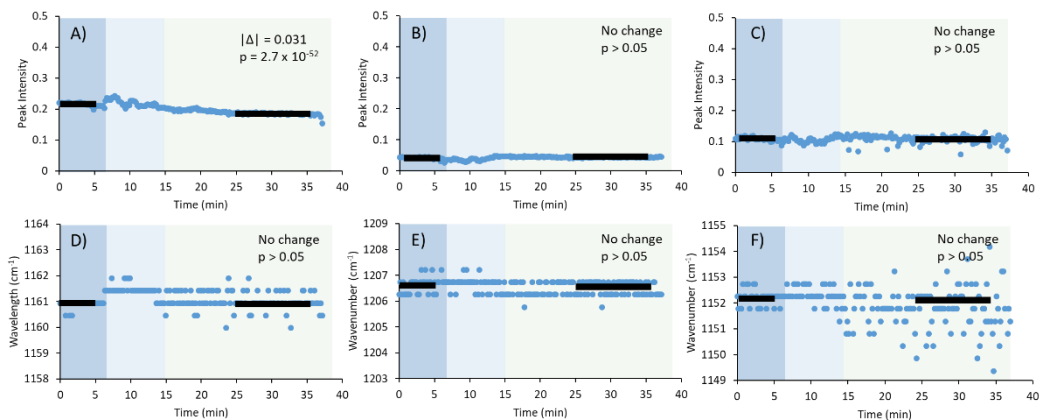


Figure S2. 5: The symmetric and asymmetric vibration peaks of the glycosidic bond in cellulose centered around 1161 cm⁻¹ and 1205 cm⁻¹, respectively (A,B, and D, E). The vibration peak of the anomeric C1-O bond centered at around 1153 cm⁻¹ (C and F). Dark bars indicate averaged regions. Absolute differences between the averaged regions ($|\Delta|$) and the p -value indicating the t -statistic of the difference are shown ($p < 0.01$ are considered significant). Colored regions corresponding to Figure S2.1 indicate fully hydrated (dark blue), drying (light blue) and fully dried (green) periods in the experiment.

References

- Jarvis, M. C. (2023). Hydrogen bonding and other non-covalent interactions at the surfaces of cellulose microfibrils. *Cellulose*, 30(2), 667–687. <https://doi.org/10.1007/s10570-022-04954-3>
- Lee, C. M., Kubicki, J. D., Fan, B., Zhong, L., Jarvis, M. C., & Kim, S. H. (2015). Hydrogen-Bonding Network and OH Stretch Vibration of Cellulose: Comparison of Computational Modeling with Polarized IR and SFG Spectra. *The Journal of Physical Chemistry B*, 119(49), 15138–15149. <https://doi.org/10.1021/acs.jpcc.5b08015>
- Marechal, Y., & Chanzy, H. (2000). The hydrogen bond network in Ib cellulose as observed by infrared spectrometry. *Journal of Molecular Structure*, 14.
- Newman, R. H., & Davidson, T. C. (2004). Molecular conformations at the cellulose–water interface. *Cellulose*, 11(1), 23–32. <https://doi.org/10.1023/B:CELL.0000014778.49291.c6>

Viëtor, R. J., Newman, R. H., Ha, M.-A., Apperley, D. C., & Jarvis, M. C. (2002). Conformational features of crystal-surface cellulose from higher plants. *The Plant Journal*, 30(6), 721–731. <https://doi.org/10.1046/j.1365-313X.2002.01327.x>